

Climatic control of denudation in the deglaciated landscape of the Washington Cascades

Seulgi Moon^{1*}, C. Page Chamberlain², Kimberly Blisniuk³, Nathaniel Levine¹, Dylan H. Rood⁴ and George E. Hilley¹

Since the Last Glacial Maximum, the extent of glaciers in many mountainous regions has declined, and erosion driven by glacial processes has been supplanted by fluvial incision and mass wasting processes. This shift in the drivers of erosion is thought to have altered the rate and pattern of denudation of these landscapes. The Washington Cascades Mountains in the northwestern USA still bear the topographic imprint of Pleistocene glaciations, and are affected by large variations in precipitation, making them an ideal setting to assess the relative controls of denudation. Here we show that denudation rates over the past millennia, as determined by ¹⁰Be exposure ages, range from 0.08 to 0.57 mm yr⁻¹, about four times higher than the rates inferred for million-year timescales. We find that the millennial timescale denudation rates increase linearly with modern precipitation rates. Based on our landscape analyses, we suggest that this relationship arises because intense precipitation triggers landslides, particularly on slopes that have been steepened by glacial erosion before or during the Last Glacial Maximum. We conclude that the high modern interglacial denudation rates we observe in the Washington Cascades are driven by a disequilibrium between the inherited topography and the current spatial distribution of erosional processes that makes this range particularly sensitive to spatial variations in climate.

Before ~11–17 kyr ago (ref. 1), cirque and valley glaciers were pervasive in the Washington Cascades, and deglaciation has resulted in steep valley side slopes and wide valley bottoms inherited from the previous action of alpine valley glaciers (Fig. 1a; refs 2,3). With glacial recession, fluvial incision and mass wasting processes now denude the oversteepened parts of deglaciated landscape (for example, hanging valleys and steep side walls of glacial valleys)^{2,4,5}. The Cascades features a factor-of-ten variation in precipitation across the range because of its orographic rain shadow⁶. Palaeobotanic studies^{7,8} and $\delta^{18}\text{O}$ of ancient meteoric water in clay minerals⁹ suggest that this rain shadow was established between 8 and 15 Myr ago. We studied thirteen basins within the upland catchments of the Washington Cascades (Fig. 1). Sampled basins were selected across the precipitation gradient with minimum lithologic variation¹⁰ to isolate the impact that climatic variations may have on the relations between denudation, topography, and climate within this landscape.

Denudation of the Cascades

We used cosmogenic ¹⁰Be concentrations from detrital river-sand samples in these basins, which were situated along an E–W transect across the Washington Cascades (Fig. 1b, Supplementary Information). Denudation rates covary strongly with precipitation, ranging from 0.08 mm yr⁻¹ to 0.57 mm yr⁻¹, whereas modern precipitation rates vary between 942 mm yr⁻¹ and 3,125 mm yr⁻¹ over the same area (Fig. 1c). Precipitation and denudation rates are linearly related and well correlated ($R^2 = 0.832$, Fig. 2a). In contrast, topographic attributes (as measured by catchment-averaged channel steepness index; K_{sn} , basin-averaged slope, mean local relief, and elevation) are not strongly correlated with denudation (Supplementary Fig. S1, Fig. 2c–e). The K_{sn} values (reference concavity 0.5; area >3 km²;

Supplementary Fig. S2) are uniformly high (2.54–2.86 for $\log_{10} K_{sn}$) and are poorly correlated with denudation (Fig. 3a), as expected in recently deglaciated landscapes¹¹ in contrast to fluvially dissected terrains^{12–14} (Supplementary Fig. S3). Local relief (elevation range over a 10-km-diameter circular area)¹⁵ also shows a relatively uniform distribution (1,222–1,599 m), whereas surface slopes increase slightly with denudation rates (Fig. 2c–e). Denudation rates are also correlated with average slopes and local relief at the 5-km scale (Fig. 2c,e), but less strongly than with precipitation (Fig. 2a). Precipitation and denudation show large variations from basin to basin (a factor-of-three variation in basin-averaged precipitation, and a factor-of-seven variation in denudation). Basin-averaged long-term denudation rates inferred from apatite (U–Th)/He (A–He) analyses vary from ~0.03 mm yr⁻¹ to 0.22 mm yr⁻¹ in the study area¹⁶ and short-term denudation from cosmogenic isotopes are ~4 times higher than long-term denudation rates from A–He analyses (Fig. 2b).

Denudation rates inferred from the abundance of ¹⁰Be in river-sands represent post-glacial denudation, as denudation rates provided by this method are averaged over the time it takes to erode ~0.6 m of rock, which is equivalent to ~1.1–7.4 kyr of denudation in this landscape. As the last glaciations in this area ceased by ~11–17 kyr ago (ref. 1), most of our samples should largely reflect post-recessional denudation (Supplementary Fig. S4; refs 17,18), although as we discuss below, inherited topographic variations from previous glacial episodes may modulate denudation rates. In addition, the preferential erosion of glacial deposits from these basins may strongly bias the denudation rates we infer. Although such a hypothesis is difficult to completely dismiss in any environment, the large variation in ¹⁰Be inventories observed in catchments measured across the entire range is disproportionate to the variation in the

¹Department of Geological and Environmental Sciences, Stanford University, Building 320, Room 306D, 450 Serra Mall Stanford, California 94305, USA,

²Department of Environmental Earth System Sciences, Stanford University, Stanford, California 94305, USA, ³Department of Geology, University of California, Davis, California 95616, USA, ⁴Lawrence Livermore National Laboratory, Center for Accelerator Mass Spectrometry, Livermore, California 94551, USA. *e-mail: sgmoon@stanford.edu.

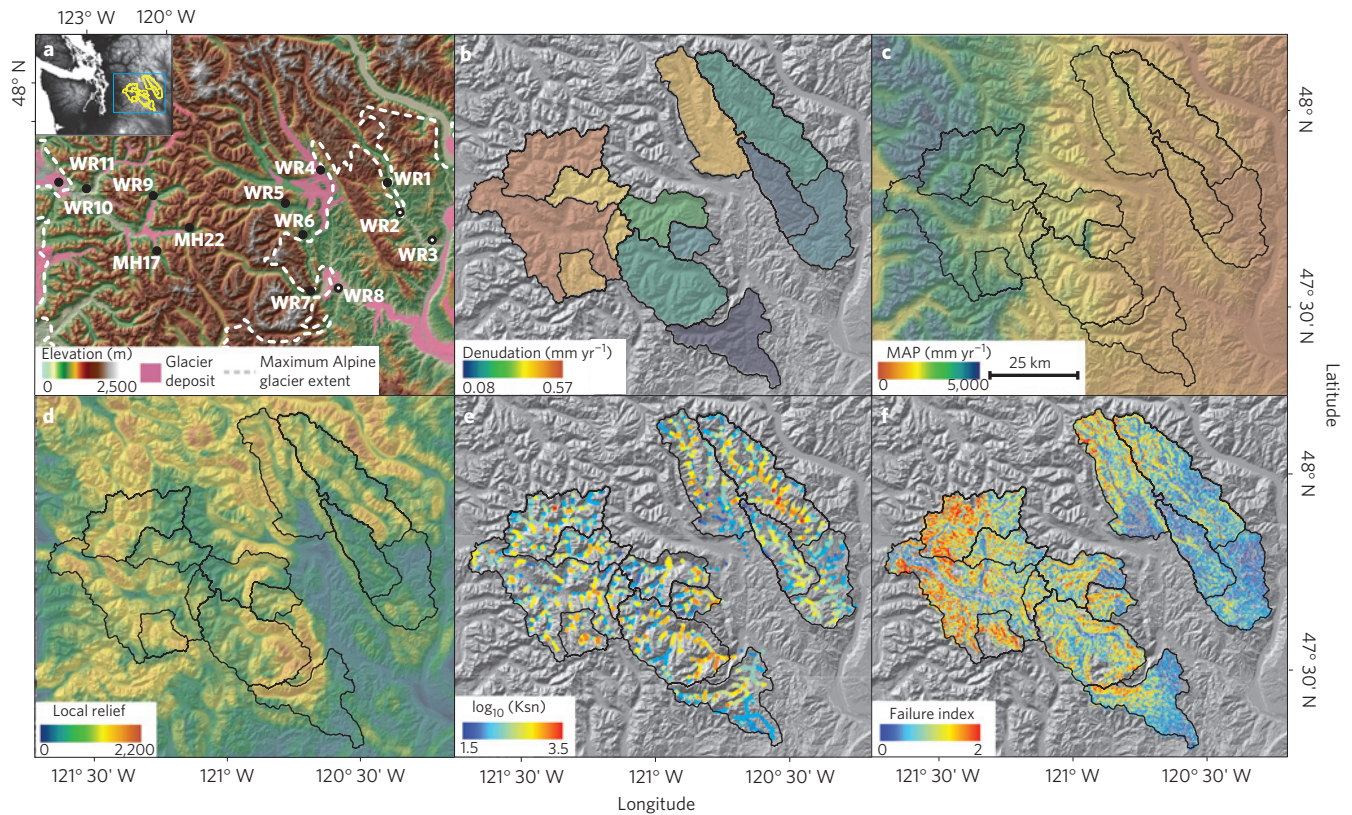


Figure 1 | Map of the Washington Cascades. **a**, Digital elevation map with inset map of the western USA. Inset map shows a blue box for the study area of Reiners *et al.*¹⁶ and basins in yellow for this study. Glacial deposits are shown as red regions¹⁰, the maximum alpine glacier extent as a white dotted line², black dots and open circles indicate sample locations (WR and MH). **b**, Sample basins colour-coded by ¹⁰Be denudation rates. **c**, Mean annual precipitation (MAP; 1971–2000; ref. 6). **d**, Local relief from a 5-km-diameter circular window. **e**, Channel steepness (K_{sn}) with area >3 km². **f**, Failure index.

area of glacial deposits present within each of the catchments¹⁰. For these features to substantially impact the denudation rates we measured, the relative contribution of sediments sourced from these features must both be large and change systematically with precipitation (Supplementary Fig. S5); thus, the systematic trend in denudation observed across the range is unlikely to arise from erosion of these features. Finally, it is unlikely that enhanced short-term denudation rates arise from recent secular changes in tectonic rock uplift rates. The scarcity of Quaternary faults and seismicity in the Cascades suggests that recent tectonic activity in this area has been limited over the past several million years (Fig. 1b; <http://earthquake.usgs.gov/hazards/qfaults>), although limited exposure of geologic structures in this landscape may have obscured identification of these features. This area has had a documented, recent, and profound change in the distribution of erosional processes, but lacks the observed active structures necessary to accommodate the accelerated fault movement that might produce short-term increases in denudation. Thus, it seems reasonable that the changes we resolve probably result from geomorphic process changes accompanying glaciation and glacial recession (Supplementary Information).

Interestingly, long-term denudation measured previously in this area also correlates with precipitation, which led Reiners *et al.*¹⁶ to conclude that the processes that uplift rocks in this range might be controlled by long-term climate patterns. In this case, denudation limits or reduces topography and lithostatic stresses, allowing uplift to be localized in areas where erosional unloading is rapid^{16,19}. The higher recent rates must be fairly short-lived (<~2.6 Myr), otherwise the samples reported by Reiners *et al.*¹⁶ would necessarily have younger A–He cooling ages (Supplementary Information).

Such apparent enhanced short-term denudation rates relative to long-term averages have been observed in environments subjected

to cyclic glacial–interglacial changes in erosional processes^{3,18,20}. According to a glacial erosion study in the Coast Mountains in British Columbia²¹, a rapid increase in glacial denudation occurred when the glaciers initially excavated the valley at 1.8–1.4 Myr ago, but once the glacial relief structure was established, there seemed to be limited incision of existing valleys. In the Cascades, glaciation seems to have been established by Plio–Quaternary time, if not earlier^{1,22}. If the rapid valley deepening observed in the Coast Mountains is a typical response to the onset of glaciation, denudation rates averaged throughout the Quaternary may be different from those inferred from A–He ages. However, recent denudation rates we infer from ¹⁰Be analyses probably record denudation processes that greatly postdate this initial phase of excavation. Continued valley widening by glacial action may also accelerate denudation rates over the Quaternary; however, when using a minimum duration for glaciation in the area and a restoration of narrow, pre-glacial valley geometries, we estimate that valley widening can only account for ~0.005–0.045 mm yr⁻¹ of average denudation over this time period (Supplementary Fig. S6). Given that much of the denudation associated with the onset of glaciations may have occurred in the Pliocene or early Quaternary and valley widening cannot account for the rapid short-term denudation rates we resolve, it seems most plausible that the rapid ¹⁰Be-derived denudation rates are related to changes in erosional processes that accompany deglaciation of the area.

Role of past glaciations in modulating modern denudation

We used topographic analyses to explore the role that pre- and post-recessional conditions may play in increasing denudation rates and producing covariation between current denudation and precipitation rates. First, we examined the imprint of

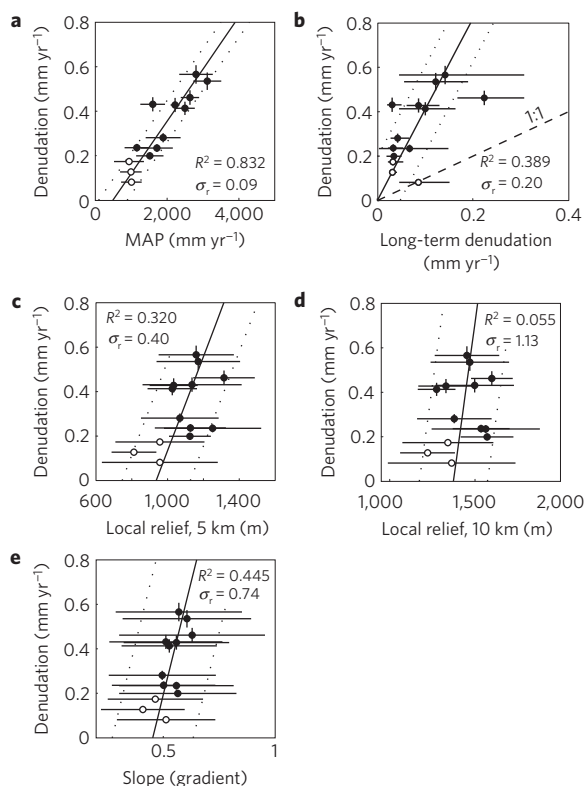


Figure 2 | Plot of climatic and topographic parameters with denudation rate. **a**, Precipitation rate. **b**, Long-term denudation rate inferred from apatite A–He measurements. **c**, Local relief from a 5 km-diameter window. **d**, Local relief from a 10 km window, and **(e)** basin-averaged slope. Samples collected from basins with a limited glacial extent are denoted by open circles (WR2, 3 and 8). Error bars for denudation rates represent 1σ uncertainty in measured ^{10}Be concentration, minimum to maximum range in long-term denudation rates, 1σ standard deviation in precipitation, local relief and slope within sample basins. Uncertainties in regressions denote 1σ residual error (σ_r) of linear fit.

spatial variations in precipitation on the relief structure of the former glaciated range. We compared two reliefs calculated using 5-km- and 10-km-diameter circular windows with measured denudation rates. The relief calculated using a 10-km-diameter window captures the elevation difference between peaks and valley bottoms of large glacial valleys. Along the western side of the Cascades, this scale measures relief within areas of the landscape that were pervasively subjected to the action of glaciers in the past. However, along the eastern side of the range, the large valleys were occupied by through-flowing glaciers originating in the higher-precipitation area to the west, whereas the upland area was not scoured by glaciers because of lower precipitation in these areas (WR2, 3, and 8, the areas of which were less than 75% glaciated, are shown as open circles in Figs 1–3).

The 10-km-diameter sampling window does not discriminate between areas dominated by past glacial erosion versus fluvial incision along the eastern side of the range, and as a result, local relief computed at this scale varies little across the study area and is uncorrelated with denudation ($R^2 = 0.055$, Fig. 2d). In contrast, relief calculated over a 5-km-diameter window discriminates between basins in the east that were not previously glaciated and those with mainstem valleys that were sculpted by glaciers (Fig. 1d). The presence of low relief, smaller catchments along the eastern slope of the Cascades, and the absence of these features to the west suggests that orographic precipitation during the Last Glacial

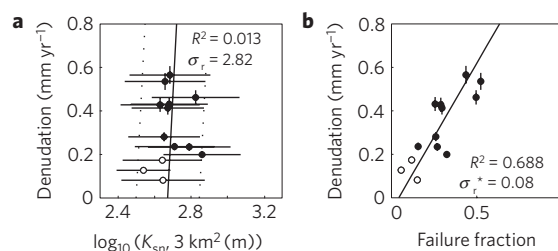


Figure 3 | Plot of denudation rate with metrics for the denudation process. **a**, K_{sn} from channel points with basin area $>3 \text{ km}^2$, which represents channel incision processes, and **(b)** failure fraction from channel points with basin area $<1 \text{ km}^2$, which represents the fraction of points expected to be dominated by shallow landslides. Error bars represent 1σ standard deviation in K_{sn} within sample basins, and 1σ uncertainty in measured ^{10}Be concentration in denudation rates.

Maximum probably affected the past extent of glaciers, especially along the eastern side of the Cascades. Local relief computed over a smaller window scale correlates moderately with denudation rate ($R^2 = 0.320$, Fig. 2c), suggesting that the relief asymmetry created by past differences in glacial extent across the range influences denudation rates to some degree.

Processes that facilitate recent, rapid denudation

Next, to evaluate those erosional processes probably responsible for the recent acceleration of denudation and the covariation of denudation and precipitation, we first computed average channel steepness within basin areas $>3 \text{ km}^2$ (ref. 23). This metric was used to gauge the relative voracity of river incision across the landscape²⁴. As expected for recently deglaciated topography¹¹, denudation rate and channel steepness are poorly correlated with one another, suggesting that the elevated denudation rates we observe do not seem to be derived from increased river incision (Figs 1e, 3a, Supplementary Information). Second, we used a version of the infinite slope approximation for failure of a cohesionless frictional material coupled to a steady-state hydrologic model to predict the relative susceptibility of different areas to erosion by shallow landslides²⁵. Points with basin areas $<1 \text{ km}^2$ were isolated for this analysis, and the fraction of points expected to fail as landslides was determined for each basin (hereafter referred to as the failure fraction; Figs 1f, 3b, Supplementary Information). Denudation rates increase systematically with the failure fraction. Both slopes and precipitation rate affect the relative susceptibility of hillslopes to landsliding, and these factors systematically change by varying degrees across the Cascades. We evaluated their relative contributions to slope failure by varying precipitation across the range with slope fixed to the mean value, and then varying slope across the range while precipitation rate was fixed to its mean value. Although both are probably important in triggering slope failure, denudation rates correlate most strongly with the failure fraction when slope is fixed, and secondarily to the failure fraction when precipitation is fixed (Supplementary Fig. S7). This suggests that increases in pore pressure owing to current rainfall gradients across the Cascades, and secondarily the variations in slopes across the range created before the last deglaciation, cause shallow landslides to denude basins in the west more vigorously than their drier counterparts.

Implications for denudation rates in deglaciated landscapes

In contrast to our findings, others have found that ^{10}Be -derived denudation rates show little, if any, correlation with precipitation^{26,27}. This may be owing to the fact that the Cascades experienced a recent, profound change in the erosional processes

that erode this landscape. In contrast, the landscapes examined in these previous studies may have been only moderately perturbed by the glacial–interglacial transition, and as such, they may maintain an approximate balance between denudation and rock uplift^{19,28}. In these areas, landscape forms are in balance with time-invariant tectonic, climatic, and lithologic factors, and the pace of denudation is matched to rock uplift²⁹. In contrast, the topographic forms of the Washington Cascades reflect relict glacial erosion processes rather than those that currently denude the landscape², and as a result, denudation rates in this disequilibrium landscape seem strongly correlated with spatial variations in climate (for example, ref. 30).

That said, there are recently deglaciated landscapes that do not show the clear relationship between denudation rates and precipitation that we resolve in the Cascades^{3,18,31}. Cosmogenically measured denudation rates in the Central Alps are well-correlated with topographic attributes but not mean annual precipitation¹⁸. In the Cascades, the landscape has a greater precipitation gradient, has a more uniform slope distribution, and is restricted to a smaller area of homogeneous lithologies than present in the Alpine study area^{3,18}. As we have shown earlier, the glacial relief structure that was imaged using various local relief measurements covaries with spatial changes in precipitation rates to some degree. This covariation may allow a clearer relationship between denudation and precipitation to be resolved here. However, these variations in slope are much smaller than for the Alps, in which slope is a strong explanatory factor of denudation¹⁸. Thus, it seems that the strong precipitation gradient, relatively uniform lithology, and weak variations in slopes across the range have allowed us to identify a relationship between precipitation and denudation that otherwise might be difficult to detect.

We find that spatial gradients in precipitation produce a systematic increase in ¹⁰Be-measured denudation rates, and that these rates are in excess of those measured over the late Cenozoic. A physically based landslide model indicates that basins that have an increased propensity for shallow landsliding, particularly on glacially oversteepened side slopes, are also denuding rapidly. These landslides are expected to be more pervasive in areas with large amounts of precipitation relative to their drier counterparts, as well as areas with steeper slopes that were produced by precipitation-driven differences in the extent of glaciers during previous glacial periods. Our results show that denudation within the Cascades, where the topographic form is probably imbalanced with respect to the current erosional process distribution, is more rapid than the long-term average, and is susceptible to spatial variations in climate. As a result, accelerated denudation during interglacial periods may be an important contributor to the overall denudation of this range over the Quaternary.

Methods

Determination of denudation rates from ¹⁰Be concentrations. We determined denudation rates from *in situ*-produced ¹⁰Be in thirteen detrital river-sand samples collected along a transect across the Washington Cascades (Fig. 1). We intentionally focused on basins >60 km² to provide spatial averaging of discrete mass-transport processes that might otherwise render our denudation unrepresentative of a basin-wide average³². We corrected ¹⁰Be production rates for the effect of shielding of cosmic radiation by topography and snow, as well as ranges in elevations throughout the basin³³ (Supplementary Table S1). We also considered the impact of glacially modified topographic features in the calculation of denudation rates and topographic and climatic parameters, because of the fact that sediment sources would not be generated uniformly in the sample basins and small glacial lakes may impound sediment from upstream areas. To this end, we excluded areas of the landscape draining into lakes (assuming they are efficient sediment traps for the 250–710 μm size fraction) and the flat valley bottoms (assuming that sediment bypasses, but is not sourced from flat valley bottoms within this landscape). Although this modification influences our calculation of denudation rates and parameters to some degree, it does not significantly alter the relationship

between denudation and the topographic and climatic parameters investigated (Supplementary Fig. S1).

Received 31 January 2011; accepted 19 April 2011; published online 29 May 2011

References

- Porter, S. C. Pleistocene glaciation in the southern part of the North Cascade Range, Washington. *Geol. Soc. Am. Bull.* **87**, 61–75 (1976).
- Mitchell, S. G. & Montgomery, D. R. Influence of a glacial buzzsaw on the height and morphology of the Cascade Range in central Washington State, USA. *Quat. Res.* **65**, 96–107 (2006).
- Norton, K. P., Abbühl, L. M. & Schlunegger, F. Glacial conditioning as an erosional driving force in the Central Alps. *Geology* **38**, 655–658 (2010).
- Doten, C. O., Bowling, L. C., Lanini, J. S., Maurer, E. P. & Lettenmaier, D. P. A spatially distributed model for the dynamic prediction of sediment erosion and transport in mountainous forested watersheds. *Water Resour. Res.* **42**, W04417 (2006).
- Ballantyne, C. K. Paraglacial geomorphology. *Quat. Sci. Rev.* **21**, 1935–2017 (2002).
- PRISM, *United States Average Monthly or Annual Precipitation 1971–2000* (Oregon State Univ., 2006).
- Smiley, C. J. *The Ellensburg Flora of Washington* Vol. 35 (Univ. of California Publications in Geological Sciences, 1963).
- Leopold, E. B. & Denton, M. F. Comparative age of grassland and steppe east and west of the northern rocky mountain. *Ann. Missouri Bot. Garden* **74**, 841–867 (1987).
- Takeuchi, A. & Larson, P. B. Oxygen isotope evidence for the late Cenozoic development of an orographic rain shadow in eastern Washington, USA. *Geology* **33**, 313–316 (2005).
- Hunting, M. T., Bennett, W. A., Livingston, V. E. Jr & Moen, W. S. Geologic Map of Washington. (Washington Division of Mines and Geology, 1961).
- Brocklehurst, S. H. & Whipple, K. X. Response of glacial landscapes to spatial variations in rock uplift rate. *J. Geophys. Res.* **112**, F02035 (2007).
- DiBiase, R. A., Whipple, K. X., Heimsath, A. M. & Ouimet, W. B. Landscape form and millennial erosion rates in the San Gabriel Mountains, CA. *Earth Planet. Sci. Lett.* **289**, 134–144 (2010).
- Safran, E. B. *et al.* Erosion rates driven by channel network incision in the Bolivian Andes. *Earth Surf. Process. Landf.* **30**, 1007–1024 (2005).
- Ouimet, W. B., Whipple, K. X. & Granger, D. E. Beyond threshold hillslopes: Channel adjustment to base-level fall in tectonically active mountain ranges. *Geology* **37**, 579–582 (2009).
- Ahnert, F. Functional relationships between denudation, relief, and uplift in large, mid-latitude drainage basins. *Am. J. Sci.* **268**, 243–263 (1970).
- Reiners, P. W., Ehlers, T. A., Mitchell, S. G. & Montgomery, D. R. Coupled spatial variations in precipitation and long-term erosion rates across the Washington Cascades. *Nature* **426**, 645–647 (2003).
- Parker, G. & Perg, L. A. Probabilistic formulation of conservation of cosmogenic nuclides: Effect of surface elevation fluctuations on approach to steady state. *Earth Surf. Process. Landf.* **30**, 1127–1144 (2005).
- Wittmann, H., von Blanckenburg, F., Kruesmann, T., Norton, K. P. & Kubik, P. W. Relation between rock uplift and denudation from cosmogenic nuclides in river sediment in the Central Alps of Switzerland. *J. Geophys. Res.* **112**, F04010 (2007).
- Molnar, P. The state of interactions among tectonics, erosion, and climate: A polemic. *GSA Today* **19**, 44–45 (2009).
- Stock, G. M. *et al.* Spatial and temporal variations in denudation of the Wasatch Mountains, Utah, USA. *Lithosphere* **1**, 34–40 (2009).
- Shuster, D. L., Ehlers, T. A., Rusmoren, M. E. & Farley, K. A. Rapid glacial erosion at 1.8 Myr revealed by ⁴He/³He thermochronometry. *Science* **310**, 1668–1670 (2005).
- Haug, G. H. *et al.* North Pacific seasonality and the glaciation of North America 2.7 million years ago. *Nature* **433**, 821–825 (2005).
- Stock, J. D. & Dietrich, W. E. Erosion of steepland valleys by debris flows. *Geol. Soc. Am. Bull.* **118**, 1125–1148 (2006).
- Whipple, K. X. & Tucker, G. E. Dynamics of the stream-power river incision model: Implications for height limits of mountain ranges, landscape response timescales, and research needs. *J. Geophys. Res.* **104**, 17661–17674 (1999).
- Montgomery, D. R. & Dietrich, W. E. A physically based model for the topographic control on shallow landsliding. *Water Resour. Res.* **30**, 1153–1171 (1994).
- Riebe, C. S., Kirchner, J. W., Granger, D. E. & Finkel, R. C. Minimal climatic control on erosion rates in the Sierra Nevada, California. *Geology* **29**, 447–450 (2001).
- von Blanckenburg, F. The control mechanisms of erosion and weathering at basin scale from cosmogenic nuclides in river sediment. *Earth Planet. Sci. Lett.* **237**, 462–479 (2005).
- Willett, S. D. & Brandon, M. T. On steady states in mountain belts. *Geology* **30**, 175–178 (2002).

29. Hack, J. T. Interpretation of erosional topography in humid temperate regions. *Am. J. Sci., Bradley Volume* **258-A**, 80–97 (1960).
30. Riebe, C. S., Kirchner, J. W., Granger, D. E. & Finkel, R. C. Erosional equilibrium and disequilibrium in the Sierra Nevada, inferred from cosmogenic ^{26}Al and ^{10}Be in alluvial sediment. *Geology* **28**, 803–806 (2000).
31. Norton, K. P., von Blanckenburg, F. & Kubik, P. W. Cosmogenic nuclide-derived rates of diffusive and episodic erosion in the glacially sculpted upper Rhone Valley, Swiss Alps. *Earth Surf. Process. Landf.* **35**, 651–662 (2010).
32. Niemi, N. A., Oskin, M., Burbank, D. W., Heimsath, A. M. & Gabet, E. J. Effects of bedrock landslides on cosmogenically determined erosion rates. *Earth Planet. Sci. Lett.* **237**, 480–498 (2005).
33. Balco, G., Stone, J. O., Lifton, N. A. & Dunai, T. J. A complete and easily accessible means of calculating surface exposure ages or erosion rates from ^{10}Be and ^{26}Al measurements. *Quat. Geochronol.* **3**, 174–195 (2008).

Acknowledgements

S.M. acknowledges the support of the Stanford Graduate Fellowship and G.E.H. acknowledges the support of the Terman Fellowship. We thank T. A. Ehlers, S. D. Willet, P. W. Reiners, and K. X. Whipple for thoughtful comments.

Author contributions

S.M. designed and performed experiments, analysed data, and wrote the paper; G. E. H. and C. P. C. designed and performed experiments, and wrote the paper; K.B. and D.H.R. analysed data; and N.L. performed experiments.

Additional information

The authors declare no competing financial interests. Supplementary information accompanies this paper on www.nature.com/naturegeoscience. Reprints and permissions information is available online at <http://www.nature.com/reprints>. Correspondence and requests for materials should be addressed to S.M.